Binding of Aminoglycoside Antibiotics to the Small Ribosomal Subunit: A Continuum Electrostatics Investigation

Chiansan Ma,[†] Nathan A. Baker,*,[‡] Simpson Joseph,[§] and J. Andrew McCammon[⊥]

Contribution from the Department of Chemistry, Yale University, New Haven, Connecticut 06520, and Howard Hughes Medical Institute, Department of Chemistry and Biochemistry, and Department of Pharmacology, University of California at San Diego, 9500 Gilman Drive, La Jolla, California 92093

Received August 13, 2001

Abstract: The binding of paromomycin and similar antibiotics to the small (30S) ribosomal subunit has been studied using continuum electrostatics methods. Crystallographic information from a complex of paromomycin with the 30S subunit was used as a framework to develop structures of similar antibiotics in the same ribosomal binding site. Total binding energies were calculated from electrostatic properties obtained by solution of the Poisson–Boltzmann equation combined with a surface area-dependent apolar term. These computed results showed good correlation with experimental data. Additionally, calculation of the ribosomal electrostatic potential in the paromomycin binding site provided insight into the electrostatic mechanisms for aminoglycoside binding and clues for the rational design of more effective antibiotics.

1. Introduction

Aminoglycoside antibiotics have been studied extensively not only for their effectiveness in undermining bacterial protein synthesis, but also because knowledge of the inhibition mechanism (which reduces translational accuracy) can elucidate the mechanism of ribosomal protein synthesis itself. The action of paromomycin, and structurally related aminoglycosides such as neomycin, has been found to occur at a binding pocket adjacent to the A-site of 16S RNA in the small (30S) subunit of the bacterial ribosome.[1-5] The recent publication of atomic resolution crystal structures of the ribosome[5] has shed new light on the interaction of paromomycin analogues with this RNA binding site. The ribosome is made up of a large (50S) and small (30S) subunit and carries a very large net negative charge due to its nucleic acid composition. As a result, we can expect electrostatics to play a large part in several aspects of ribosomal function and interactions, and we can anticipate that electrostatic calculations will be an important tool in studying the process of translation.

Continuum electrostatics methods have been widely used to evaluate electrostatic contributions to binding energies in biomolecular systems.[6-10] In this study, we use the Poisson–Boltzmann equation (PBE), combined with solvent-accessible surface area models for apolar interactions, to compute the binding energies of paromomycin and similar drugs to the small ribosomal subunit. These energies are then compared with experimental values to determine the predictive power of the continuum model for the ribosome–antibiotic system. Finally, the local ribosomal electrostatic potential is analyzed to determine the relative importance of charged functional groups located throughout the antibiotic structure. The ultimate goal of this and related future studies is to obtain an accurate electrostatic model of the RNA–drug interaction, which can offer insight into future drug design as well as ribosomal structure and function.

2. Methods

Coordinates for the ribosome were obtained from the Carter et al. crystal structure of the 30S ribosomal subunit complexed with the antibiotics paromomycin, spectinomycin, and streptomycin (1FJG).[5] Hydrogens were added to the 30S crystal structure using the WHATIF program,[11] and charges and radii were assigned to the biomolecule according to AMBER force field parameters.[12] The following antibiotics were examined in this study (see Figure 1): paromomycin, ribostamycin, neamine, neomycin, and "analogues W–Z".[13,14] Coordinates from the crystal structure were altered for the purposes of functional

* To whom correspondence should be addressed.

† Yale University. E-mail: chiansan@yale.edu.

‡ Howard Hughes Medical Institute and Department of Chemistry and Biochemistry, UCSD, Mail Code 0365. E-mail: nbaker@mccammon.ucsd.edu.

§ Department of Chemistry and Biochemistry, UCSD, Mail Code 0314. E-mail: sjoseph@ucsd.edu.

⊥ Howard Hughes Medical Institute, Department of Chemistry and Biochemistry, and Department of Pharmacology, UCSD, Mail Code 0365. E-mail: jmccammon@ucsd.edu.

(1) Moazed, D.; Noller, H. F. *Nature* **1987**, *327*, 389–394.
(2) Fourmy, D.; Recht, M. I.; Blanchard, S. C.; Puglisi, J. D. *Science* **1996**, *274*, 1367–1371.
(3) Recht, M. I.; Fourmy, D.; Blanchard, S. C.; Dahlquist, K. D.; Puglisi, J. D. *J. Mol. Biol.* **1996**, *262*, 421–436.
(4) Spahn, C. M.; Prescott, C. D. *J. Mol. Med.* **1996**, *74*, 423–439.
(5) Carter, A. P.; Clemons, W. M.; Brodersen, D. E.; Morgan-Warren, R. J.; Wimberly, B. T.; Ramakrishnan, V. *Nature* **2000**, *407*, 340–348.

(6) Wong, C. F.; Hünenberger, P. H.; Akamine, P.; Narayana, N.; Diller, T.; McCammon, J. A.; Taylor, S.; Xuong, N.-H. *J. Med. Chem.* **2001**, *44*, 1530–1539.
(7) Hao, M. H.; Harvey, S. C. *Biochim. Biophys. Acta* **1995**, *1234*, 5–14.
(8) Majeux, N.; Scarsi, M.; Apostolakis, J.; Ehrhardt, C.; Caflisch, A. *Proteins: Struct., Funct. Genet.* **1999**, *37*, 88–105.
(9) Nina, M.; Berneche, S.; Roux, B. *Eur. Biophys J.* **2000**, *29*, 439–454.
(10) Mandell, J. G.; Roberts, V. A.; Pique, M. E.; Kotlovyi, V.; Mitchell, J. C.; Nelson, E.; Tsigelny, I.; Ten Eyck, L. F. *Protein Eng.* **2001**, *14*, 105–113.
(11) Vriend, G. *J. Mol. Graph.* **1990**, *8*, 52–56.
(12) Cornell, W. D.; Cieplak, P.; Bayly, C. I.; Gould, I. R.; Merz, K. M. J.; Ferguson, D. M.; Spellmeyer, D. C.; Fox, T.; Caldwell, J. W.; Kollman P, A. *J. Am. Chem. Soc.* **1995**, *117*, 5179–5197.
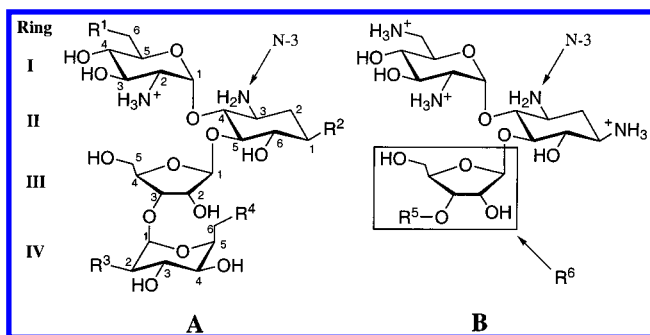
Figure 1. Structures of antibiotics used in calculations. (A) Paromomycin (R^1 = OH; R^2, R^3, R^4 = NH_3), neomycin (R^1, R^2, R^3, R^4 = NH_3), analogue Y (R^1, R^2 = NH_3; R^3, R^4 = OH), analogue Z (R^1, R^2, R^4 = NH_3; R^3 = OH). (B) Ribostamycin (R^5= H), neamine (R^6 = H), analogue W (R^5 = $(CH_2)_2$—NH_3), analogue X (R^5 = $(CH_2)_2$—NH_2—$(CH_2)_3$—NH_3).

group replacement and were otherwise unchanged. Side chains were modified within the Insight II 2000[15] software package, and the positions of modified antibiotic atoms were minimized in the presence of a subset of the 30S subunit. This 30S subset was chosen as the collection of ribosomal atoms with potential steric interactions with the antibiotic. Aminoglycoside charges were assigned to the antibiotic structures using the charge equilibration (Qeq) method[16] in the Cerius2 software,[17] and radii were assigned using AMBER parameters and atom types.[12] ^{15}N NMR studies of neomycin showed that, at physiological pH ($\sim$6.7), the N-3 amine group on ring II remains unprotonated and has a pK_a of 5.74.[18] To examine the effects of the ribosome potential on the pK_a of N-3 during binding, two different protonation states (the neutral and positively charged N-3) were calculated for each drug analogue.

Electrostatic binding energies[19] were calculated by solving the linearized PBE with the recently developed APBS (Adaptive Poisson–Boltzmann Solver) software package.[20,21] PBE calculations were performed at 298.15 K, using a 150 mM NaCl ion atmosphere with solvent and solute dielectric constants of 2.0 and 78.54, respectively. These electrostatic energies (ΔG_{elec}) were supplemented with surface area-dependent apolar contributions to give total binding energies of

$$\Delta G_{tot} = \Delta G_{elec} + \gamma \Delta A$$

where ΔA is the change in solvent-accessible surface area upon binding. The apolar constant γ was chosen with various values from 62.8 to 104.7 J mol^{-1} Å^{-2} to reflect standard (104.7) and "best-fit" (62.8) values of this parameter.[6]

To help determine the titration state of the antibiotics upon binding, pK_a shifts of the N-3 amine group were calculated. These shifts were determined in the usual fashion[22,23] by the formula

$$\Delta pK_a = \frac{\Delta G_{tot}^n - \Delta G_{tot}^p}{RT \ln 10}$$

where ΔG_{tot}^n is the binding energy calculated with a neutral N-3 group,

(13) Cashman, D. J.; Rife, J. P.; Kellogg, G. E. *Bioorg. Med. Chem. Lett.* **2001**, *11*, 119–122.
(14) Alper, P. B.; Hendrix, M.; Sears, P.; Wong, C. H. *J. Am. Chem. Soc.* **1998**, *120*, 1965–1978.
(15) *Insight II*, version 2000; Molecular Simulations, Inc., San Diego, CA, 2000.
(16) Rappe, A. K.; Goddard, W. A. I. *J. Phys. Chem.* **1991**, *95*, 3358–3363.
(17) *Cerius2*, version 3.5; Molecular Simulations, Inc., San Diego, CA, 1997.
(18) Botto, R. E.; Coxon, B. *J. Am. Chem. Soc.* **1983**, *105*, 1021–1028.
(19) Sharp, K. A.; Honig, B. *J. Phys. Chem.* **1990**, *94*, 7684–7692.
(20) Baker, N. A.; Holst, M. J.; Wang, F. *J. Comput. Chem.* **2000**, *21*, 1343–1352.
(21) Baker, N. A.; Sept, D.; Joseph, S.; Holst, M. J.; McCammon, J. A. *Proc. Natl. Acad. Sci. U.S.A.* **2001**, *98*, 10037–10041.
(22) Bashford, D.; Karplus, M. *J. Phys. Chem.* **1991**, *95*, 9556–9561.
(23) Antosiewicz, J.; McCammon, J. A.; Gilson, M. K. *Biochemistry* **1996**, *35*, 7819–7833.

ΔG_{tot}^p is the binding energy with a fully protonated N-3, R is the gas constant, and T is the temperature ($RT \ln 10 \approx 5.8$ kJ mol^{-1} at 298 K).

3. Results and Discussion

The calculated antibiotic binding energies are summarized in Table 1. These energies do not include translations and rotational entropy contributions, so only their relative values are meaningful, as discussed below. Results are given only for the N-3 uncharged state, since, as outlined below, this corresponds to the experimental conditions. Surface area change due to drug binding is also given for each drug; the calculated apolar contribution to the binding energy was calculated using the standard γ value of 104.7 J mol^{-1} Å^{-2}. The difference between energies calculated using γ values of 104.7 and 62.8 J mol^{-1} Å^{-2} is not significant, however (typically less than 5–8% of total energy). Table 1 also shows the relative binding energies $\Delta\Delta G$ calculated with respect to neomycin (the strongest binding antibiotic) by $\Delta\Delta G^{n,p} = \Delta G^{n,p} - \Delta G_{neo}^{n,p}$.

The dissociation constant (K_d) data of Alper et al.[14] were used for assessment of the calculated binding energies (see Table 1 for calculated and experimental values). These experimental data were based on the use of surface plasmon resonance to measure dissociation equilibrium constants for a fragment of the small subunit 16S RNA bound to a wide range of aminoglycoside analogues. The salt concentration used for the PBE calculations is consistent with the experimental conditions (150 mM NaCl). The Alper et al. measurements were carried out at a pH (7.4) slightly higher than physiological conditions. To match the correct pH conditions in the calculated energies, a titration state for each antibiotic must be selected. Using the experimentally calculated N-3 pK_a (5.74)[18] as a model pK_a for the antibiotic N-3 groups, Table 1 shows that none of the calculated pK_a shifts are sufficient to cause protonation of the antibiotic N-3 amines upon binding to the 30S subunit at pH 7.4. While at lower pH's (<7.0), the effects of these pK_a shifts may become more pronounced and could influence the binding properties of the antibiotics, we will assume the protonated N-3 state is not relevant for comparison with the Alper et al. experimental data. Subsequent discussion will consider only the neutral N-3 state. However, the differences in relative energies between the two states is rather small, suggesting that the effect of N-3 protonation on drug binding energy is largely independent of the structure of the rest of the molecule (data not shown). Elucidation of the titration state for the ribosome was not possible in this study and is the subject of future research; each residue or base was assigned a protonation state using its standard pK_a values and a pH of 7.4. While it is likely that some 30S titratable groups may exhibit shifted pK_a values in the ribosome interior, the good agreement of calculated values with experimental data (see below) indicates that these shifts probably do not contribute to the differing binding energies of the antibiotics considered in this study.

In Figure 2, the APBS-calculated relative binding energies are plotted against the Alper et al. experimental energies. A line with slope 0.78 ± 0.13 and intercept 2.2 ± 1.6 kJ mol^{-1} was fit to all of the antibiotic data with a correlation coefficient 0.93. However, two of the smaller antibiotics (denoted by ○ in Figure 2) clearly deviate from the rest of the data. Therefore, a second fit was performed on only the larger antibiotics (● in Figure 2), resulting in a line with slope 0.95 ± 0.19 and intercept 1.3 ± 1.7 kJ mol^{-1}, with a correlation coefficient of 0.93.

Table 1. Calculated and Experimental[14] Energies for Aminoglycoside Binding to the 30S Ribosomal Subunit[a]

antibiotic	charge	ΔG_{elec}	ΔA	ΔG_{tot}	$\Delta\Delta G_{tot}$	ΔG_{exp}	$\Delta\Delta G_{exp}$	ΔpK_a
analogue Y	+3	−14.45	−29.99	−17.59	16.18	−26.00	18.05	1.33
ribostamycin	+3	−12.29	−18.54	−14.44	19.33	−26.25	17.80	0.95
neamine	+3	−12.00	−18.54	−13.95	19.82	−29.14	14.91	0.81
analogue W	+4	−20.97	−18.54	−22.92	10.85	−32.91	11.14	1.10
analogue Z	+4	−22.83	−31.11	−26.10	7.67	−35.13	8.92	1.27
analogue X	+5	−29.88	−18.54	−31.83	1.94	−37.60	6.45	1.188
paromomycin	+4	−22.51	−31.12	−25.78	7.99	−38.23	5.82	1.04
neomycin	+5	−30.50	−31.11	−33.77	0.00	−44.05	0.00	1.20

[a] All energies are in units of kilojoules per mole, and surfaces areas are given in square angstroms. ΔG_{elec} denotes the calculated electrostatic contribution to the binding energy, ΔA is the calculated solvent-accessible surface area buried upon binding, ΔG_{tot} is the total binding energy calculated with $\gamma = 104.7$ kJ mol^{-1} Å^{-2} (see text), $\Delta\Delta G_{tot}$ is the relative calculated binding energy with respect to neomycin, δG_{exp} is the experimental binding energy, $\Delta\Delta G_{exp}$ is the relative experimental binding energy with respect to neomycin, and ΔpK_a is the calculated pK_a shift in the N-3 amine upon binding.
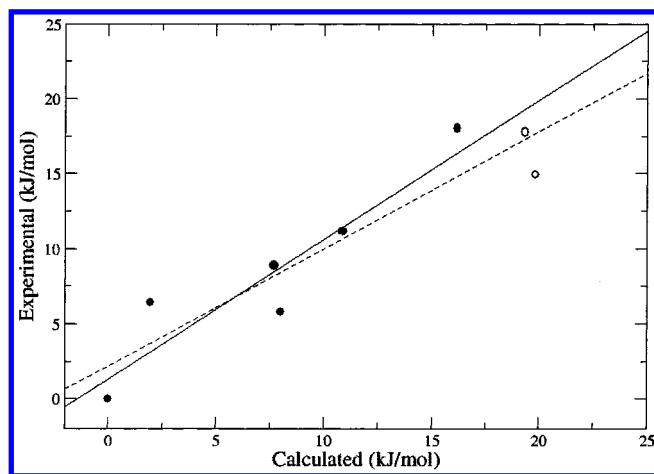

Figure 2. Experimental and calculated relative binding energies for antibiotic binding to the 30S ribosomal subunit (see text) with the N-3 amine neutral. Data points represent individual antibiotics (see Table 1) and are shown as symbols: (○) the smaller antibiotics ribostamycin and neamine; (●) the other, larger antibiotics. Least-squares fits to the data are shown as lines: the dashed line fits all of the antibiotic data, and the solid line fits only the large antibiotic data. Please refer to the text for detailed information on each fit.

These results reflect expected trends in relative binding effectiveness between different analogues: neomycin, paromomycin, and closely related analogues are more effective binders than neamine and ribostamycin. More specific correlations are also followed: for example, replacement of a charged amine with a hydroxyl group on ring IV of neomycin to produce analogue Z causes a significant drop (7.67 kJ mol^{-1}) in calculated binding energy. Replacement of a second amine on the same ring causes a more severe drop of 8.51 kJ mol^{-1}. Experimentally, similar effects (drops of 8.92 and 9.13 kJ mol^{-1}, respectively) are observed. Binding energy trends are reflected more specifically by the slope of the regression line—a slope of 1 (and corresponding intercept of 0) indicates total agreement with respect to the relative binding energies. However, with all data included, the slope of the linear regression (0.78) is somewhat less than unity. As mentioned above, this slope value is lowered by the data for neamine and ribostamycin, which deviate from the rest of the data points and are believed to be less reliable than the remainder of the data (see discussion below). Specifically, the exclusion of these smaller antibiotics yields linear fits for the remaining six with the same correlation coefficients but markedly improved slope and intercept values.

The modest deviations seen in Figure 2 can readily be explained in the context of limitations imposed on the calculations by the use of the crystal structure and neglect of conformational entropy changes. The conformations of the 30S subunit and antibiotics described by the crystal structure may differ somewhat from the actual solution conformations. Binding of the drug and RNA is assumed to occur in the manner shown in the crystal structure, but this assumption becomes less reliable as the structure of the tested molecule diverges from that of paromomycin. In particular, ribostamycin and neamine do not contain all four of the rings found in paromomycin (see Figure 1). To facilitate reasonably rapid evaluation of the binding energies, the calculation assumed no deviations in the ribosomal structure from the 30S−paromomycin conformation when antibiotics other than paromomycin were bound. The deviation of the ribostamycin and neamine energies might well result, in part, from this discrepancy. The other tested drug analogues consist of four rings or three rings and a carbon chain in place of the fourth ring; here, the crystal structure is likely to be more accurate in describing binding. Additional discrepancies could arise from the failure of the present study to explicitly include entropic contributions due to conformational flexibility in the antibiotic molecules. Presumably, the loss of conformational, rotational, and translation freedom of the antibiotic makes binding less favorable. The conformational component of this energy contribution should be more significant for the larger ligands with more degrees of freedom. This argument is supported by the excellent fit to experimental data when only antibiotics of similar size are considered. Future work could incorporate recent advances[24] for quantitatively treating such entropy losses upon binding.

Because APBS treats only the electrostatic aspects of hydrogen bonding, less accurate results may be expected in cases where drug binding depends more heavily on hydrogen bonds. For example, APBS calculates less accurate energies for paromomycin than neomycin; ring I of paromomycin is stabilized by hydrogen bonding of its 6-OH hydroxyl group with nearby base A1408, while in neomycin, this hydroxyl is replaced with a protonated amine, whose contribution is more electrostatic in nature. Similarly, ribostamycin and neamine lack the electrostatic interactions provided by the charged amines on rings III and IV. In the absence of these interactions, hydrogen bonds play a greater role in ribostamycin and neamine binding; the inaccuracy in calculated energies might then be a result of incomplete treatment of hydrogen bonding as well as a lack of conformational flexibility.

Evaluation of the accuracy of the calculations is somewhat uncertain as well, as the experimental binding energies of aminoglycosides to 16S RNA have not been definitively

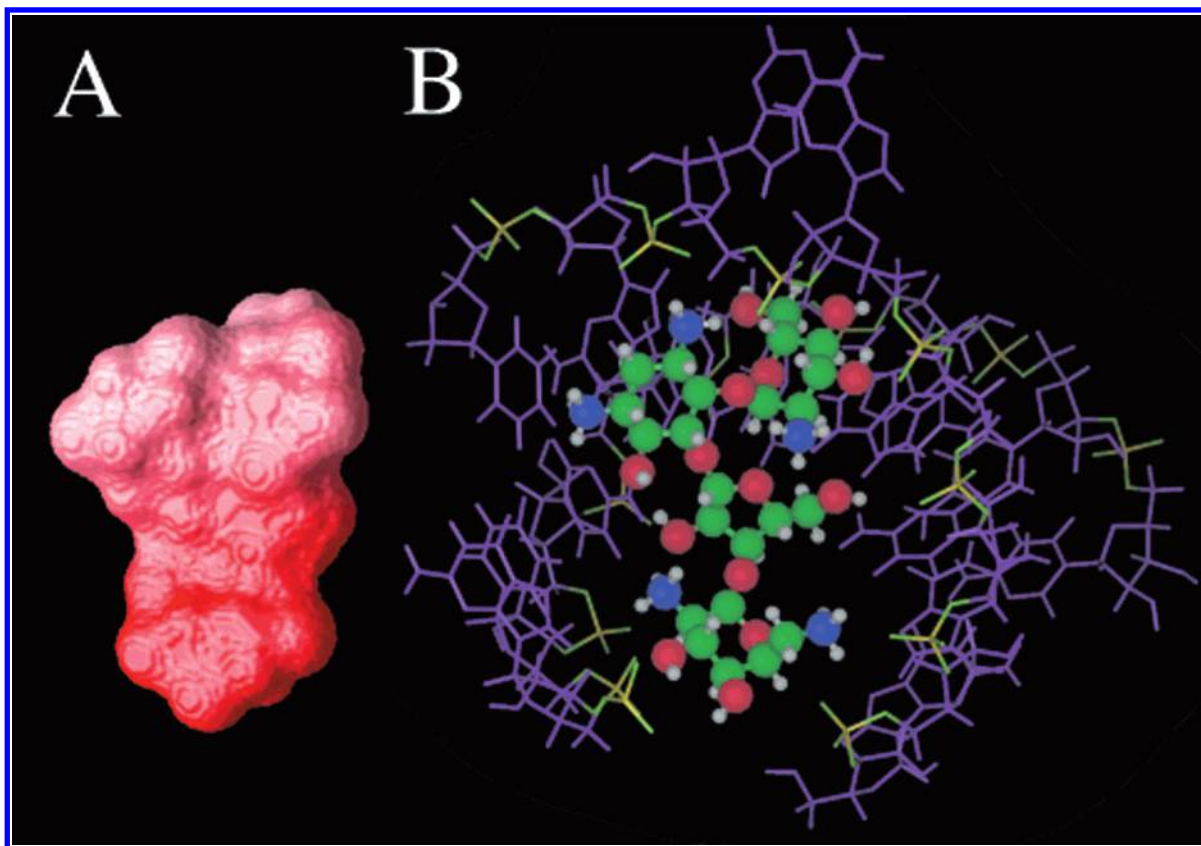(24) Noskov, S. Y.; Lim, C. *Biophys. J.* **2001**, *81,* 737−750.

Figure 3. Local environment of 30S subunit near the paromomycin binding site. (A) 30S electrostatic potential mapped onto paromomycin molecular surface (white, 0 kT/e; red, 0−5 kT/e). (B) Paromomycin (ball-and-stick) in 30S binding site with neighboring 16S rRNA (shown in purple, phosphate groups in green and yellow). No protein atoms are present in the immediate vicinity of the binding site; the nearest peptide is S12, located roughly 5 Å from ring I of the antibiotics.

established. The dissociation constants (K_d) of various aminoglycosides bound to small RNA binding site models have been measured by several different methods, including electrospray ionization mass spectroscopy[25] and fluorescence anisotropy,[26] as well as the surface plasmon resonance methods used by Alper et al.[14] Little direct comparison between methods is possible, however, as few studies have been conducted under the same solution conditions. It is also possible that the charge and radii parameters could influence the results. A subset of the above molecules was run with several different parameter sets. While the absolute binding energy values showed substantial deviation between parameter sets, the trends in binding energy were typically preserved. Likewise, the choice of the *linearized* Poisson−Boltzmann equation for electrostatics may also affect the accuracy of the results. Conventional wisdom and the physics underlying Poisson−Boltzmann theory both suggest that the *nonlinear* Poisson−Boltzmann equation is most appropriate for highly charged biomolecules such as the ribosome. Therefore, it is somewhat surprising that the results of this study show such good agreement with experiment. Nevertheless, the correlation between the APBS calculations and the Alper data is very encouraging.

Having established the ability of continuum electrostatics methods such as the PBE to predict antibiotic binding energies, we are in a position to elucidate the structural components of

paromomycin-like antibiotics which contribute favorably to 30S binding. Figure 3 depicts the electrostatic potential of the small ribosomal subunit mapped onto the molecular surface of paromomycin. Not surprisingly, the potential in the paromomycin binding site is predominantly negative; Figure 3 shows that the drug binding environment is far more negative at one end of the antibiotic molecule. The ribosomal potential around rings I and II is between −1 and −2 kT/e, approximately −3 kT/e on ring III, and assumes values of −5 kT/e and below on ring IV. The composition of the paromomycin binding site explains the intensity of the negative potential around the drug molecule (see Figure 3): rings III and IV are surrounded primarily by the negatively charged phosphate groups of the RNA backbone, while rings I and II attach to the 30S through hydrogen bonding to neighboring nucleotides as well as charge interactions. This observation suggests that charged antibiotic functional groups in rings III and IV are most effective in increasing drug affinity for the binding site. A similar observation was made by Cashman et al.[13] in their hydropathic analysis of aminoglycoside antibiotics. Binding site affinity might be increased further in drug analogues with more positive charge on rings III and IV. Such new analogues might be produced by replacement of the two hydroxyl groups on ring IV with amines; both of these groups are axial, so repulsion between the amines might be avoided. Another possibility is the placement of charge on ring III, which is neutral and thought to serve mainly as a connection between rings II and IV. The addition of other cationic groups, such as guanidine, might also be considered

(25) Wong, C. H.; Hendrix, M.; Priestley, E. S.; Greenberg, W. A. *Chem. Biol.* **1998**, *5,* 397−406.
(26) Sannes-Lowery, K. A.; Griffey, R. H.; Hofstadler, S. A. *Anal. Biochem.* **2000**, *280,* 264−271.

(guanidinylation has been observed to increase the effectiveness of aminoglycosides as HIV replication inhibitors[27,28]). Of course, too much alteration of the structure might result in a different equilibrium conformation of the binding site, one that does not bring about the desired changes in ribosomal function; the shape of the binding site as it interacts with the antibiotic must be a consideration in drug design as well.

4. Conclusions

Recent developments in methodology and software for electrostatics calculations have opened the door to computational investigation of the large-scale structures, such as the ribosome, which have been resolved by modern crystallographic techniques. By calculating electrostatic potentials in active sites and drug binding regions, it is possible to discover where and how ligands might be effectively modified to increase electrostatic affinity and drug action. In this paper, we have used information on the 30S paromomycin binding site to test the interactions between the 30S and a wide range of antibiotics. The calculated binding energies showed good agreement with experimental data and provide useful information on placement of charged functional groups on the paromomycin scaffold for future drug design. Additionally, the calculations give insight into the extent to which the aminoglycoside structure can be varied while the binding site conformation remains fixed.

Future work will focus on the improvement of these types of calculations for large biomolecules such as the ribosome.

(27) Luedtke, N. W.; Baker, T. J.; Goodman, M.; Tor, Y. *J. Am. Chem. Soc.* **2000**, *122*, 12035−12036.
(28) Baker, T. J.; Luedtke, N. W.; Tor, Y.; Goodman, M. *J. Org. Chem.* **2000**, *65*, 9054−9058.

Such improvements will likely involve solution of the nonlinear PBE rather than the linearized model used in these studies. The nonlinear PBE offers the ability to provide a more accurate description of ion distributions and electrostatic potential around highly charged systems. While the protonation states of the drug molecules are fairly well established, further work is required to elucidate with certainty the protonation state of the ribosome. The negatively charged environment provided by the ribosome almost certainly affects the protonation of protein (and possibly RNA) titratable groups. Because protonation cannot be determined directly from crystal structures, calculation of the protonation states of the ribosome (particularly near sites critical to protein synthesis) will be a major step toward understanding ribosomal function.

Supporting Information Available: Coordinates, charges, and radii for the aminoglycoside antibiotics used in this work (PDF). This material is available free of charge via the Internet at http://pubs.acs.org.

JA016830+